A Comparison of Hydrostatic and Nonhydrostatic Wave-CISK

G. W. KENT MOORE

Department of Physics, University of Toronto, Toronto, Ontario, Canada M5S 1A7

(Manuscript received 2 July 1984, in final form 11 January 1985)

ABSTRACT

Most conventional wave-CISK models have been used in the study of circulations with aspect ratios less than one, and as a result have been hydrostatic. In general, the most unstable waves in the models are the small-scale high frequency ones. For these waves the hydrostatic assumption is invalid. It therefore seems appropriate to consider a model in which the high aspect ratio waves are treated correctly, i.e., a nonhydrostatic one. In this paper, a comparison between a hydrostatic and a nonhydrostatic wave-CISK model is made. In the hydrostatic model, there is no coupling of the horizontal and vertical scales of the waves and this results in its lack of scale selection. The nonhydrostatic model has an explicit coupling in it and this leads to a preferred scale for the growth of the waves. For all the cases considered, the most unstable wave has an aspect ratio of order one.

1. Introduction

The organization of convection by larger-scale circulations is an active area of research in meteorology. In the 1960s, it was hypothesized that a cooperative interaction between the cumulus and larger-scale circulations could result in the intensification and organization of the convection. This process has been called conditional instability of the second kind, or CISK. The first example of its use was the Ekman-CISK model of tropical cyclogenesis proposed by Ooyama (1964), and Charney and Eliassen (1964). They hypothesized that the low-level convergence due to a surface Ekman layer was responsible for the cumulus convection. Inherent in the model was an interaction between the large-scale flow, which provided the moisture needed for convection, and the cumulus clouds, which provided the heating that drove the large-scale flow. Results showed that Ekman-CISK was capable of producing unstable modes. However, in the absence of viscosity, there was no scale selection.

Ekman pumping is an important source of low-level convergence for large-scale systems such as hurricanes. For internal-gravity and other waves, there exists the possibility that the convergence of the wave itself is sufficient to produce CISK. This parameterization, called wave-CISK, has been investigated by numerous authors, including Hayashi (1970), Lindzen (1974), and Chang (1976a). Hayashi, in his study of wave-CISK on an equatorial β-plane, found unstable waves that were analogues of internal-gravity, Kelvin, mixed Rossby-gravity and Rossby waves. However, the most unstable waves in the system were the small-scale gravity waves. In addition, these waves had very short periods, and hence should have been inefficient in lifting parcels from the boundary layer to the level of free convection. This problem with very unstable, short scale, high frequency waves was common to all early wave-CISK models.

Various attempts have been made to overcome these difficulties. Hayashi (1971) used a frequency dependent heating field. By reducing the heating induced by the short period waves, he was able to stabilize the small scale high frequency gravity waves. The study suffered from the lack of a physical mechanism responsible for the frequency dependence. Kuo (1975) suggested that the rate at which moisture could be supplied was the limiting constraint on the growth of the waves. Chang (1976b) suggested that Kuo's constraint was, in fact, a high frequency filter, related to the finite time required to lift an air parcel from the boundary layer to the level of free convection. This modification to the wave-CISK parameterization was used by Moore (1983) in his study of the organization of convection in the narrow cold-frontal rainband. Davies (1979) proposed that the time lag between the low-level convergence and the initiation of convection was responsible for filtering out the high frequency waves. Those waves with periods less than the time lag between the convergence and the convection would not produce any significant heating, and hence would not be excited.

Much of the work described above has been used in the study of circulations with aspect ratio less than one and as a result the models have been hydrostatic. In spite of this *a priori* assumption about the scales of interest, the models have their most unstable solutions in the high aspect ratio regime, where the hydrostatic assumption is invalid. It therefore seems

appropriate to consider a model in which the high aspect ratio waves are treated correctly, i.e., a nonhydrostatic one. As will be shown, the key drawback to the hydrostatic models is that the efficiency of the waves at CISK is not a function of their horizontal scale. In fact, most of the modifications described herein (Hayashi, 1971; Davies, 1979; Moore, 1983) attempt in some *ad hoc* fashion to introduce scale dependence into the model. In the nonhydrostatic model, the dependence is explicit and leads to a preferred scale for the growth of the waves. In this paper, a comparison of hydrostatic and nonhydrostatic wave-CISK models will be made. This study originated out of the author's research into the mesoscale organization of midlatitude convection and as a result, the analysis will be carried out on a nonrotating, shallow Boussinesq mean state. The theory for the two models will be developed in Section 2. In Section 3, the solutions in the hydrostatic model will be considered, while in Section 4 the analysis will be repeated with the nonhydrostatic model. A comparison of the two models and their implications for the study of mesoscale circulations will be made in Section 5.

2. Model theory

a. The eigenvalue problem

Consider the following system of equations for two-dimensional perturbations on a shallow Boussinesq mean state at rest:

$$\left.\begin{aligned} \frac{\partial U'}{\partial t} &= -\frac{1}{\rho_0}\frac{\partial P'}{\partial x} \\ \epsilon\frac{\partial W'}{\partial t} &= -\frac{1}{\rho_0}\frac{\partial P'}{\partial z} - \frac{\rho' g}{\rho_0} \\ \frac{\partial \rho'}{\partial t} &= \frac{\rho_0}{g}N^2 W' - \frac{\rho_0}{g}Q' \\ \frac{\partial W'}{\partial x} &+ \frac{\partial W'}{\partial z} = 0 \end{aligned}\right\}. \tag{1}$$

The flag ϵ indicates whether or not the perturbations are hydrostatic. The quantity Q' denotes the amount of heat released or absorbed by the system. To close the system, one must express Q' in terms of the other perturbation fields.

The simplest model is obtained if we allow Q' to be proportional to W'. That is:

$$Q'(x, z, t) = \alpha^* N^2 W'(x, z, t).$$

The model is unstable only if $\alpha^* > 1$, and in this case it reduces to that of perturbations on an unstably stratified mean state. The growth rates increase as the scale of the perturbations decrease. As pointed out by Lilly (1960), the growth rates in the hydrostatic limit are unbounded. With the inclusion of nonhydrostatic effects, they asymptote to the magnitude of the effective unstable Brunt-Väisälä frequency.

A more sophisticated model is obtained if one assumes that the heating is proportional to the vertical velocity at some boundary layer height and that it is distributed between the level of free convection and the top of the convective layer according to some prescribed distribution. In other words:

$$\begin{aligned} Q'(x, z, t) &= \alpha N^2 W'(x, z_0, t) f(z), \quad z_c < z < H, \\ &= 0, \quad z < z_c, \quad z > H; \end{aligned}$$

where z_0, z_c, H are the boundary layer reference level, level of free convection, and depth of convection respectively, and α is the Boussinesq diabatic heating amplitude multiplied by g/C_pT_0. The analysis of the model with this parameterization, the so-called wave-CISK model, is the subject of this paper.

A normal mode expansion of the form:

$$\begin{pmatrix} U'(x, z, t) \\ P'(x, z, t) \\ W'(x, z, t) \\ \rho'(x, z, t) \end{pmatrix} = \sum_k \begin{pmatrix} U(z) \\ P(z) \\ W(z) \\ \rho(z) \end{pmatrix} e^{i(kx-\omega t)}$$

reduces the problem to an ordinary differential equation for $W(z)$:

$$W_{zz} + \lambda^2 W = \alpha(\epsilon k^2 + \lambda^2) f(z) W(z_0), \tag{2}$$

where the vertical wavenumber λ is defined as:

$$\lambda^2 = \frac{k^2}{\omega^2}(N^2 - \epsilon\omega^2).$$

To close the problem, we will assume that the eddy vertical velocity vanishes at $z = 0$, and that at the top of the convective layer the vertical energy flux is positive. That is:

$$\begin{aligned} W(z = 0) &= 0 \\ W(z \geq H) &\approx e^{-i\lambda z}, \quad \mathrm{Re}\lambda > 0. \end{aligned} \tag{3}$$

The solution to the eigenvalue problem for ω, equations (2) and (3), can be found by Green's Method. It is:

$$W(z) = \alpha(\epsilon k^2 + \lambda^2) W(z_0) \int_0^\infty G(z, z') f(z') dz', \tag{4}$$

where:

$$\begin{aligned} G(z, z') &= -\frac{1}{\lambda}\sin\lambda z e^{-i\lambda z'}, \quad z < z' \\ &= -\frac{1}{\lambda}\sin\lambda z' e^{-i\lambda z}, \quad z > z'. \end{aligned}$$

For the solutions to be consistent, i.e. the waves that induce the heating are those excited by it, (4) must reduce to an identity at the boundary layer depth z_0. In nondimensional form (4) at $z = z_0$ is:

$$1 = -\alpha\left(\frac{\epsilon k^2 + \lambda^2}{\lambda}\right)\sin\delta\lambda \int_\gamma^1 f(z')e^{-i\lambda z'}dz' \quad (5)$$

where δ is the scaled boundary layer depth z_0/H, and γ is the scaled level of free convection z_c/H. The nondimensional horizontal wavenumber k is proportional to the aspect ratio, H/L, of the wave. Solutions to (5) give λ as a function of k and the convective parameters. The complex frequency ω is then obtained from:

$$\omega^2 = \frac{k^2N^2}{\epsilon k^2 + \lambda^2}. \quad (6)$$

b. Energetics

The energy relations for the eddies can be obtained from the linearized system (1). They are:

$$\frac{\partial}{\partial t}\int\int \frac{U'^2 + \epsilon W'^2}{2}dxdz = -\int\int \frac{g}{\rho_0}\rho' W' dxdz - \frac{[W'P']}{\rho_0}\infty,$$

$$\frac{\partial}{\partial t}\int\int \frac{1}{2}\frac{g^2}{\rho_0^2}\frac{\rho'^2}{N^2}dxdz = \int\int \frac{g}{\rho_0}\rho' W' dxdz - \int\int \frac{g}{\rho_0}\frac{\rho' Q'}{N^2}dxdz.$$

The waves are forced by the cumulus heating term S_q defined by:

$$S_q = -\int\int \frac{g}{\rho_0}\frac{\rho' Q'}{N^2}dxdz,$$

and grow by conversion of eddy potential energy into eddy kinetic energy through the buoyancy conversion term C_b defined by:

$$C_b = -\int\int \frac{g}{\rho_0}\rho' W' dxdz.$$

A necessary and sufficient condition for instability is that

$$S_q > C_b > 0. \quad (7)$$

Bolton (1980) showed that for unstable wave-CISK solutions, the heating field must somewhere be out of phase with the vertical velocity field. An understanding of the importance of this result can be obtained by considering the energy constraints on the waves. If one assumes the following decomposition of the vertical velocity field:

$$W(z) = |W|e^{i\theta}, \quad |W| \text{ and } \theta \text{ are functions of } z; \quad (8)$$

then the energy conversion terms have the following form:

$$S_q = \omega_i \int (Q^2 - Q|W|\cos\theta)dz + \omega_r \int Q|W|\sin\theta dz,$$

$$C_b = \omega_i \int (Q|W|\cos\theta - |W|^2)dz + \omega_r \int Q|W|\sin\theta dz.$$

The condition for instability, (7), reduces to the following inequality:

$$\omega_i \int (Q|W|\cos\theta - |W|^2)dz > \omega_r \int Q|W|\sin\theta dz. \quad (9)$$

Consider the special case where the vertical velocity is in phase with the heating, i.e., $\theta = 0$. Then (9) simplifies to:

$$\int Q|W|dz > \int |W|^2 dz.$$

If Q is of order α_0 and W is of order W_0, then unstable solutions are possible only if

$$\alpha > W_0 \approx 4.$$

Therefore unstable solutions with W in phase with Q exist only for large values of the heating amplitude. In this regime the model is identical to that of exponentially growing perturbations excited on an unstably stratified mean state. For smaller values of the heating amplitude, unstable solutions will exist only if W is somewhere out of phase with Q, i.e., $\theta > 0$. It is these solutions that are commonly called the wave-CISK solutions. For small values of α there are no unstable solutions that satisfy (9), regardless of the relative phase between W and Q.

3. The Hydrostatic wave-CISK model

In the hydrostatic model, the horizontal scale dependence drops out of the characteristic equation (5) and it reduces to:

$$1 + \alpha\lambda \sin\delta\lambda \int_\gamma^1 f(z')e^{-i\lambda z'}dz' = 0, \quad (10)$$

with

$$\omega^2 = \frac{k^2N^2}{\lambda^2}.$$

There are multiple roots to (10) for a given set of convective parameters. There are branches of solutions: the H_1 mode with $\lambda_r \sim 2\pi$, the H_2 mode with $\lambda_r \sim 4\pi$ and so on. Due to the complicated dependence of W on λ, as contained in equation (4), one cannot infer the vertical structure of the waves from the magnitude of λ. However, the modes with larger λ_r tend to have smaller vertical scales and they will be excited only if the vertical heating distribution, $f(z)$, has significant power at these scales. Lindzen (1974) used a constant vertical heating distribution

and encountered this problem. To deal with it, he assumed that those waves with vertical scales less than the height of the level of free convection would be inefficient at inducing any heating and would *a posteriori* be ignored. The observed heating profiles in the tropics (Chang, 1976a) are sinusoidal in shape with a maximum in the middle troposphere, and for these profiles the higher modes are not excited. Typically only the first two modes are unstable. Based on the observations summarized by Chang (1976a), a sinusoidal heating profile $f(z) = \sin\pi z$ was used. The most important convective parameter is the magnitude of the heating amplitude α and, as was shown in Section 2b, the nature of the solutions depends critically on its value. For simplicity, the nondimensional boundary layer depth and the level of free convection δ and γ were fixed at 0.1. Figures 1 and 2 show the growth rates and frequencies of the first two modes as a function of aspect ratio and heating amplitude α.

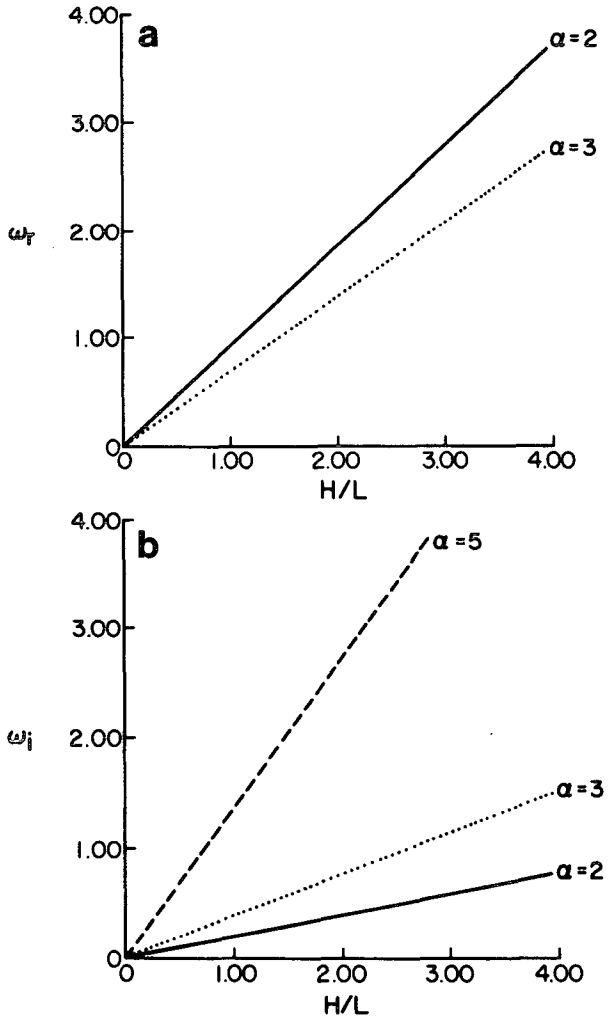

FIG. 1. (a) Nondimensional frequency ω_r and (b) growth rate ω_i of the H_1 mode as a function of aspect ratio H/L. The curves are labeled with values of the heating amplitude α.

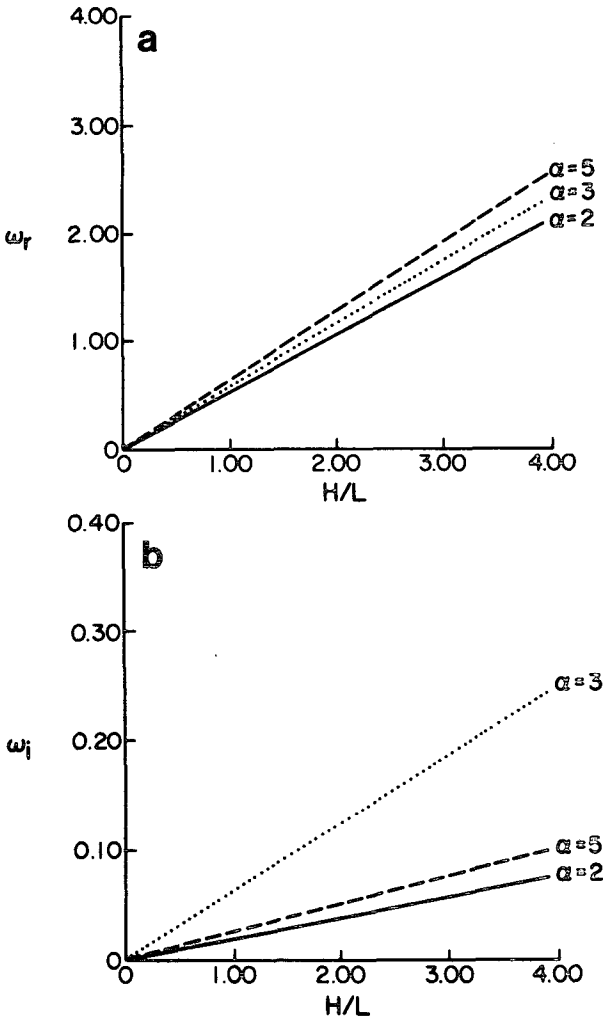

FIG. 2. As in Fig. 1 but for the H_2 mode.

For a given heating amplitude, the growth rates of the waves increase linearly with aspect ratio H/L. In the limit of large aspect ratio, i.e., small horizontal scale, the growth rate is unbounded. This behavior is also observed for hydrostatic perturbations in an unstably stratified environment. If one ignores the boundary flux term and scales the eddy energy equation

$$\frac{\partial}{\partial t}(K_H + P_E) = -S_q,$$

then one can show that:

K_H, P_E (hydrostatic eddy kinetic and potential energy) $\approx (H/L)^{-2}$,

S_q (cumulus heating term) $\approx (H/L)^{-1}$.

Therefore, the large growth rates of the small-scale waves are the result of the small hydrostatic energies

at these scales. Herein lies the problem with simple hydrostatic models of convection, namely that the smallest scales are the most unstable. Obviously the hydrostatic approximation is invalid for these scales, and when it is dropped the eddy energy is modified so as to include a contribution from the vertical velocity. As a result, the nonhydrostatic kinetic energy is finite in the small-scale limit, and this leads to an upper bound on the growth rates. In the unstably stratified model, there is still no scale selection as the growth rates asymptote to the magnitude of the unstable Brunt-Väisälä frequency. In the wave-CISK model, the behavior is more complicated and will be dealt with in Section 4.

For a given aspect ratio the growth rate generally increases with increasing α. This is not the case for large heating amplitudes in the H_2 mode, where the growth rate decreases with increasing α. For each mode there is a minimum heating amplitude for instability. For the convective parameters used, $\alpha_{\min} \sim 1.2$ for the H_1 mode and $\alpha_{\min} \sim 1.6$ for the H_2 mode. For each mode, heating amplitudes larger than the minimum result in unstable solutions. The waves are forced by the heating field and, as it becomes more intense, their vertical structure will become similar to that of the heating field. As a result, the phase shift between W and Q will tend to zero. For these waves one can define an effective stratification parameter α^* by:

$$\alpha^* = \alpha / W_0,$$

where W_0 is the magnitude of the vertical velocity field. The waves will be unstable only if $\alpha^* > 1$ and will be similar to perturbations excited on an unstably stratified mean state. Figures 3 and 4 show the magnitude and phase of the vertical velocity field, as defined by (8), of the H_1 and H_2 modes as a function of α.

For the H_1 mode, the neutral waves have a unimodal structure with a maximum at a lower level than that of the heating field. The unstable waves are characterized by a relatively constant positive phase-shift between W and Q at intermediate levels, and a negative phase tilt at upper levels (this tilt being due to the radiation condition at the upper boundary). As the heating amplitude increases, the positive phase shift diminishes and above $\alpha \sim 4.2$ it is identically zero. In this regime the perturbations have α^* greater than one and the growth rates increase with increasing α.

A similar behavior is observed for the H_2 modes for heating amplitudes less than 3.2. The neutral waves in the mode have a bimodal structure which evolves into a unimodal structure as α increases. For $\alpha > 3.2$, the phase shift between W and Q is very small and the waves have α^* less than one. The nonzero growth rates are the result of the small

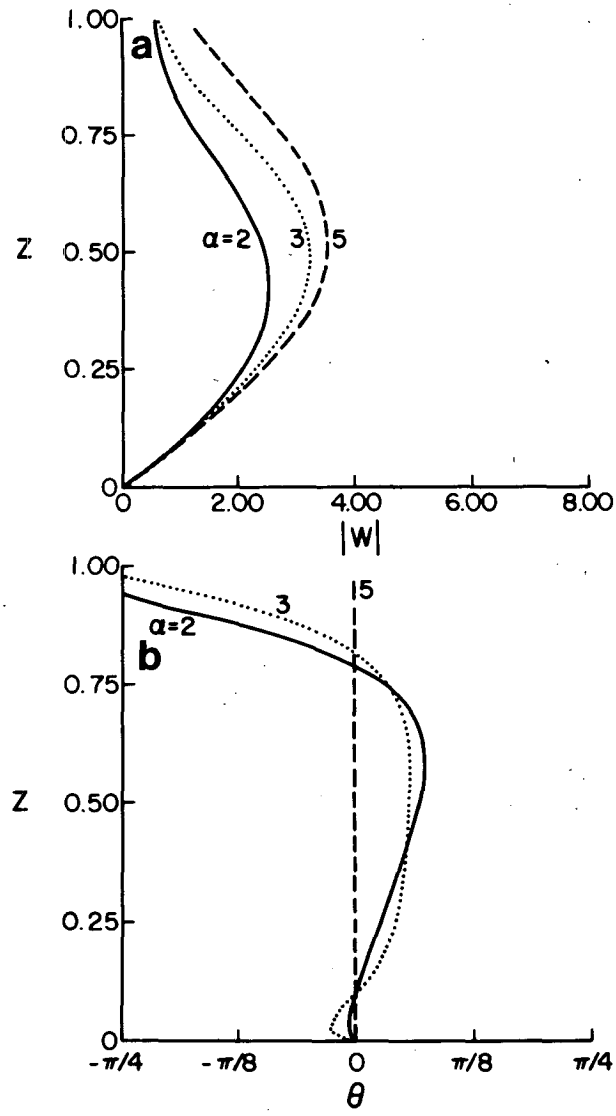

FIG. 3. (a) Magnitude and (b) relative phase of the vertical velocity field of the H_1 mode. The curves are labeled with values of the heating amplitude α. The vertical scale is normalized by the depth of convection H and the magnitude of W is normalized so that $W(z_0) = 1$. The phase is relative to the prescribed heating distribution.

amount of heat released at upper levels where W and Q are out of phase.

In summary, for a sinusoidal heating field there were two unstable modes. Both suffered from a lack of scale selection; that is, the shortest scales were the most unstable. Each mode had a minimum heating amplitude for instability. As α was increased from these minima, the vertical structure of the waves became similar to that of the heating field. For large values of the heating amplitude, the phase shift between W and Q in both modes went to zero. In this regime the H_1 mode was characterized by an effective unstable stratification and the growth rates

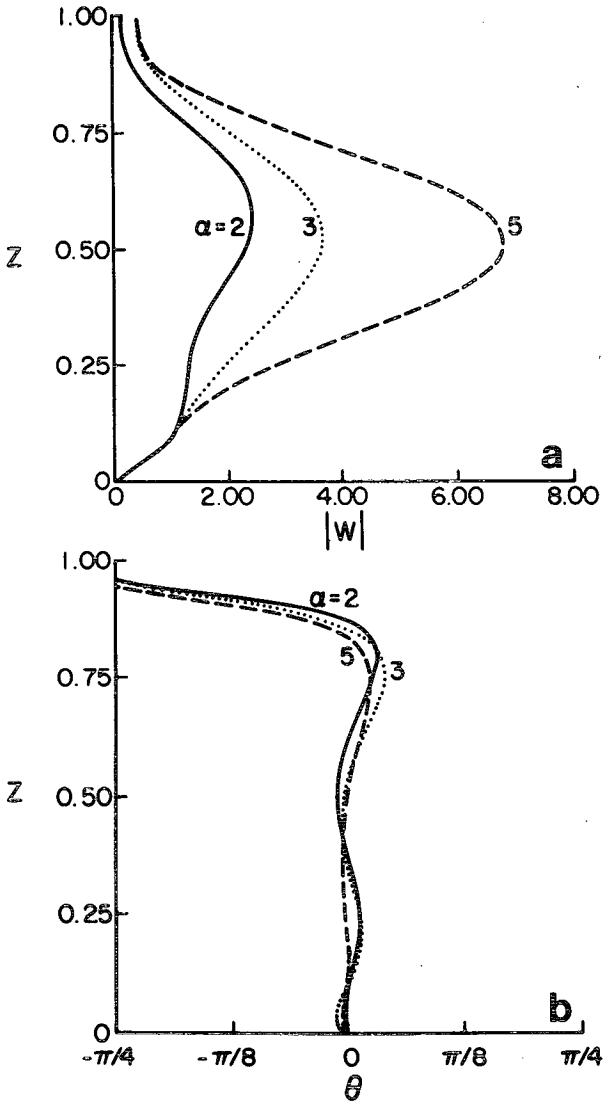

FIG. 4. As in Fig. 3 but for the H_2 mode.

increased with increasing α, while the H_2 mode had an effective stable stratification and the growth rates decreased with increasing α.

4. The nonhydrostatic wave-CISK model

In the nonhydrostatic model, the efficiency of the waves at CISK is a function of their horizontal scale, and this has profound implications on the behaviour of the model for intermediate- and short-scale waves. In the nonhydrostatic model, the characteristic equation is:

$$1 + \alpha\left(\frac{k^2 + \lambda^2}{\lambda}\right)\sin\delta\lambda \int_\gamma^1 f(z')e^{-i\lambda z'}dz = 0, \quad (11)$$

with

$$\omega^2 = \frac{k^2N^2}{k^2 + \lambda^2}.$$

As in the hydrostatic model, there are multiple roots to this equation. The picture is complicated by the fact that λ is a function of k. If one identifies the modes by their behaviour in the limit $k = 0$, then there are branches of solutions: the NH_1 mode with $\lambda_r \sim 2\Pi$; the NH_2 mode with $\lambda_r \sim 4\pi$; and so on. The higher modes are not excited when a sinusoidal heating profile is used.

Recall that in the hydrostatic model the growth rates increased with decreasing horizontal scale. As was shown in the previous section, this was due to the neglect of the vertical velocity component in the eddy kinetic energy. This led to an underestimation of the kinetic energy of the small-scale waves and resulted in their unbounded growth rates. The nonhydrostatic model includes this term in its energy budget and results in upper bounds for the growth rates. In the hydrostatic model, the vertical structure of the waves is the same for all horizontal scales and comparison of (10) and (11) shows that it is identical to the $k = 0$ limit of the nonhydrostatic model. That is, the structure of the waves in the hydrostatic model, and hence their efficiency at CISK, is fixed by the behavior of the large-scale $k = 0$ waves. The nonhydrostatic model, with its dependence of λ on the horizontal scale of the waves, does not suffer from this problem.

The first result of this scale dependence is that the minimum heating amplitude for instability is a function of aspect ratio. That is, there are unstable intermediate- and short-scale waves for values of α below the minima for instability in the hydrostatic model. Figure 5 shows the growth rates and frequencies of the waves in the NH_1 and NH_2 modes as a function of H/L for $\alpha = 1$. The long waves in both modes are stable, as predicted by the hydrostatic theory, while the intermediate- and short-scale waves are unstable. In both modes there is a most unstable aspect ratio.

For heating amplitudes larger than the minima in the hydrostatic model, the long waves are unstable. Figure 6 shows the growth rates and frequencies of the NH_1 and NH_2 modes as a function of H/L for $\alpha = 2$. As in the low heating regime, both modes have a preferred scale of the growth of the waves. Figures 7 and 8 show the vertical structure of the waves in the two modes as a function of aspect ratio. The evolution of the waves as the aspect ratio is increased is very similar to that observed in the hydrostatic mode as α was increased. As the scale of the waves decreases, the phase shift between W and Q decreases and in the limit of large aspect ratio both modes have an effective α^* less than one. As a result, in the small-scale limit the waves have low growth rates.

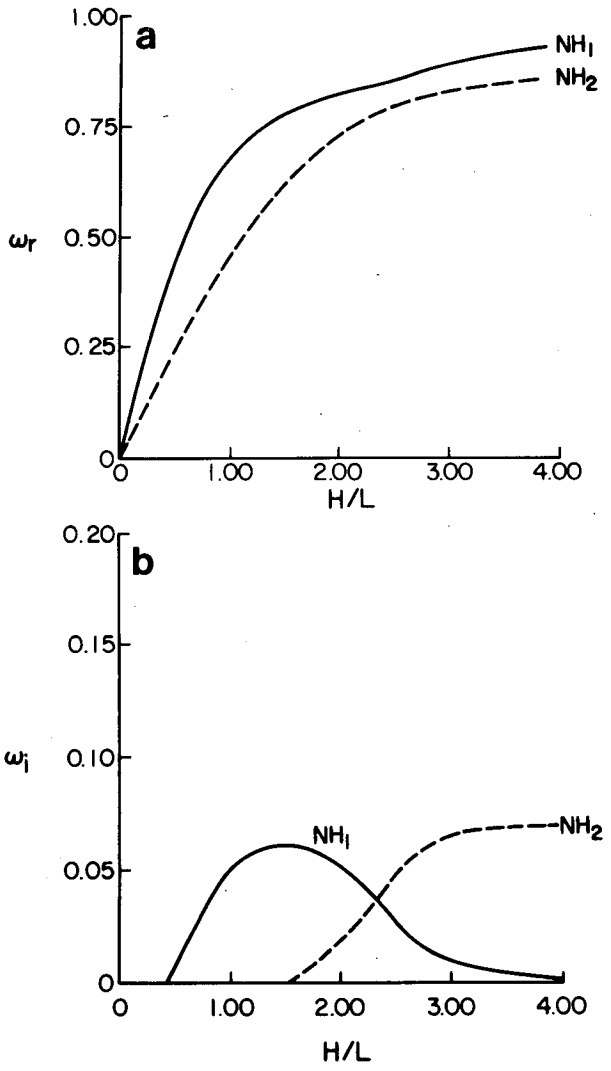

FIG. 5. (a) Nondimensional frequency ω_r and (b) growth rate ω_i of the NH_1 and NH_2 modes for $\alpha = 1$.

In Figure 9, the growth rates and frequencies of the waves in the NH_1 and NH_2 modes as a function of H/L are shown for $\alpha = 5$. Recall that the hydrostatic H_1 and H_2 modes in this regime had W in phase with Q and as a result one could define an effective stratification α^* for the modes. The H_1 mode had $\alpha^* > 1$ and was unstable, while the H_2 mode had $\alpha^* < 1$ and was quasi-stable. The long waves in the NH_1 mode also have W in phase with Q but unlike the H_1 modes, α^* is a function of their horizontal scale. This results in a preferred scale for the growth of the waves. The shorter scale waves in the mode have a positive phase shift between W and Q. There is an abrupt transition in the behavior of the waves; the long waves are stationary with the vertical velocity in phase with the heating, while the shorter waves are propagating with a positive phase shift between W and Q. For all waves in the NH_2 mode, α^* is less than one and as a result the growth rates are small.

As previously described, each mode had a preferred scale for the growth of the waves. As the heating amplitude increased, the wavelength of the most unstable wave in each mode shifted to longer scales. For α less than 2.5 the most unstable wave was associated with the NH_2 mode, while for α greater than 2.5 it was associated with the NH_1 mode. Although there was a transition in the most unstable mode as α increased, the vertical structure of the most unstable waves were quite similar. This is shown in Fig. 10. In all cases the phase shift between W and Q was constant through the middle levels of the convective layer and as α increased, it went to zero. Therefore, as the heating became more intense, there was a transition from a propagating most unstable wave with $\theta > 0$ to a stationary one with $\theta = 0$. Figure 11 shows the vertical structure of the secondary

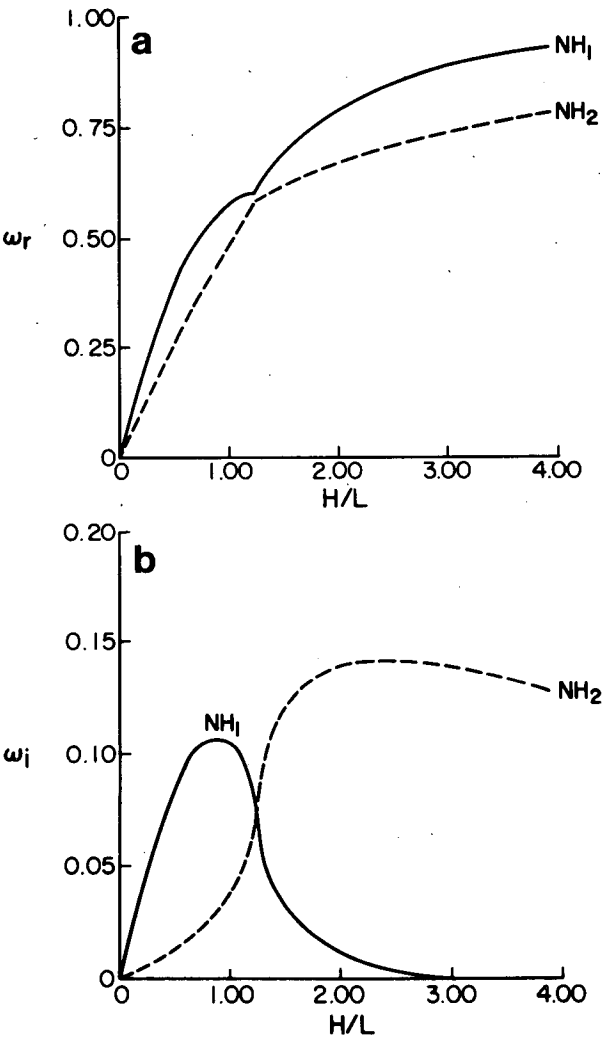

FIG. 6. As in Fig. 5 but for $\alpha = 2$.

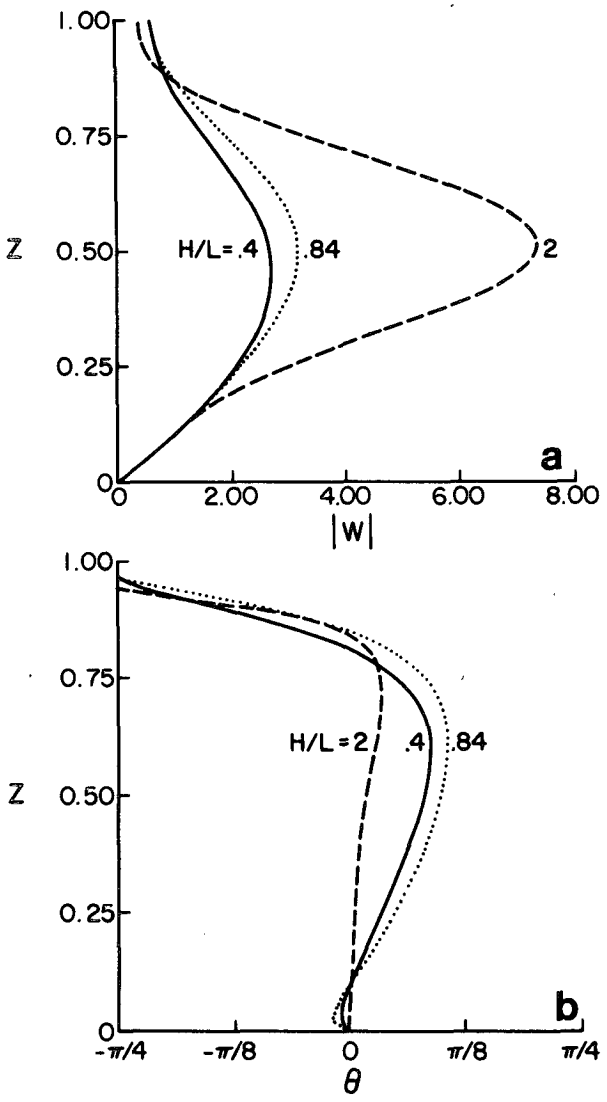

FIG. 7. As in Fig. 3 but for the NH_1 mode for $\alpha = 2$. The curves are labeled with values of the aspect ratio H/L.

most unstable wave as a function of α. Unlike the structure of the primary wave, the phase shift between W and Q is concentrated at middle levels. For $\alpha < 2$ there was little difference in the growth rates of the two most unstable waves. In this regime the longer NH_1 wave had higher phase and group velocities than the shorter NH_2 wave.

In summary, the inclusion of nonhydrostatic effects resulted in the efficiency of the waves at CISK to be a function of their horizontal scale. For both unstable modes, this resulted in a preferred scale for the growth of the waves. For the cases considered, the most unstable waves had an aspect ratio of order one. For heating amplitudes less than 2, the growth rates of the two most unstable waves were the same order. As the heating amplitude was increased the growth rates of the two waves became disparate and there was a single most-unstable wave. Above $\alpha = 4.2$, this wave had the vertical velocity field in phase with the heating.

5. Discussion

In this paper I have compared models of hydrostatic and nonhydrostatic wave-CISK. In the CISK parameterization, one attempts to relate the release of latent heat due to convection to the vertical velocity of the waves at some level in the boundary layer. A realistic treatment of the vertical velocity field of the waves is therefore crucial. The validity of the hydrostatic approximation depends on the aspect ratio of the flow. For $H/L < 1$, the particle motions will be essentially horizontal with the vertical velocity determined by

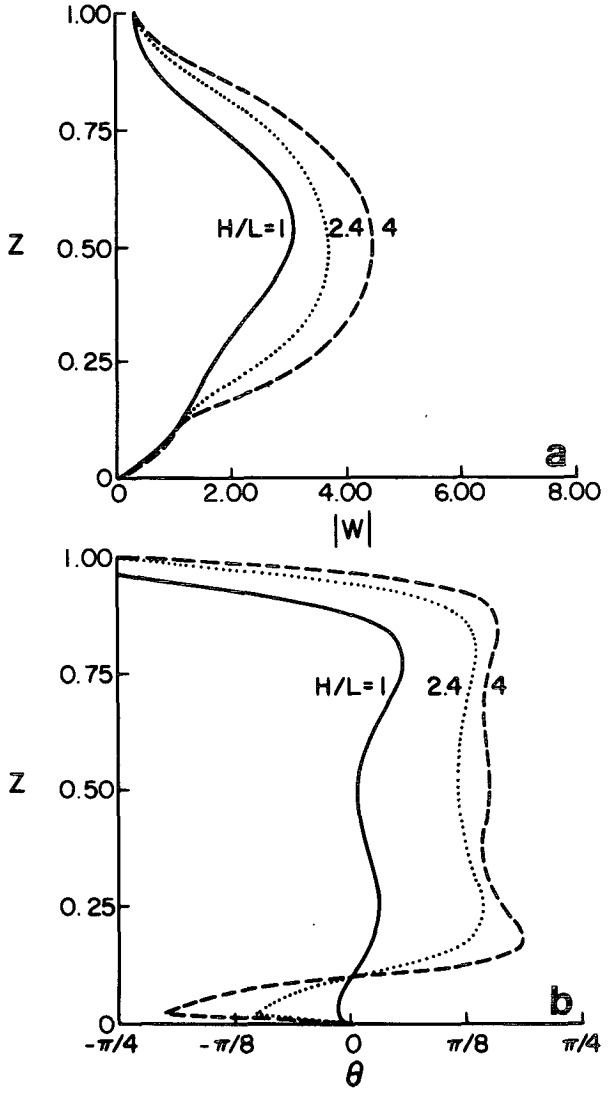

FIG. 8. As in Fig. 7 but for the NH_2 mode.

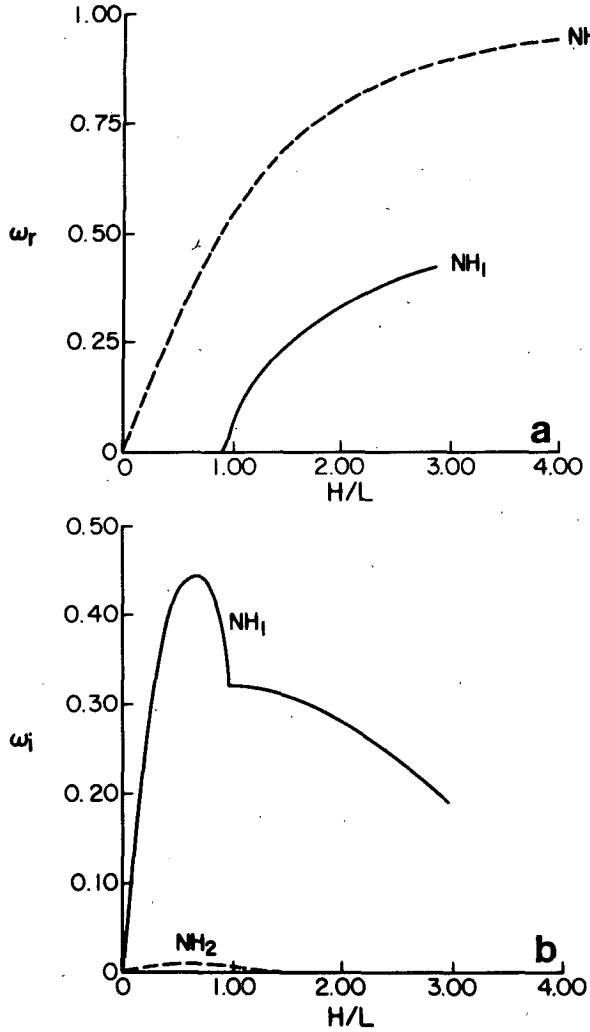

FIG. 9. As in Fig. 5 but for $\alpha = 5$.

the horizontal convergence field alone. If the horizontal and vertical scales of the flow are commensurate, i.e., $H/L \gtrsim 1$, then the vertical acceleration term cannot be ignored with respect to the vertical pressure gradient and buoyancy terms. The dynamic determination of W has profound effects on behavior of the wave-CISK model.

The hydrostatic model suffered from a lack of scale selection. In particular, the growth rate was a linear function of the aspect ratio. The slope was determined by the convective parameters, most notably the heating amplitude α. Analysis of the energetics showed that the lack of scale selection was the result of the eddy energy tending to zero more rapidly than the cumulus heating term. For large values of the heating amplitude the vertical velocity field was in phase with the heating field. In this limit the stability of the waves depended on an effective stratification parameter α^*. For the H_1 mode, α^* was greater than one and it was unstable, while for the H_2 mode α^* was less than one and the mode was quasi-stable.

In the nonhydrostatic model, the efficiency of the waves at CISK was a function of the horizontal scale of the waves. In the short wave limit, the waves had α^* less than one and hence the waves were quasi-stable. For heating amplitudes less than the minimum required for instability in the hydrostatic model, there were unstable intermediate- and short-scale waves. Both unstable modes had a preferred scale with aspect ratio of order 1 for the growth of the eddies. For low heating amplitudes the most unstable waves in the two modes had about the same growth rates, while for high heating amplitudes the most unstable wave was associated with the NH_1 mode. Although the maxima in both modes shifted to longer scales as the heating increased, the vertical structure of the most

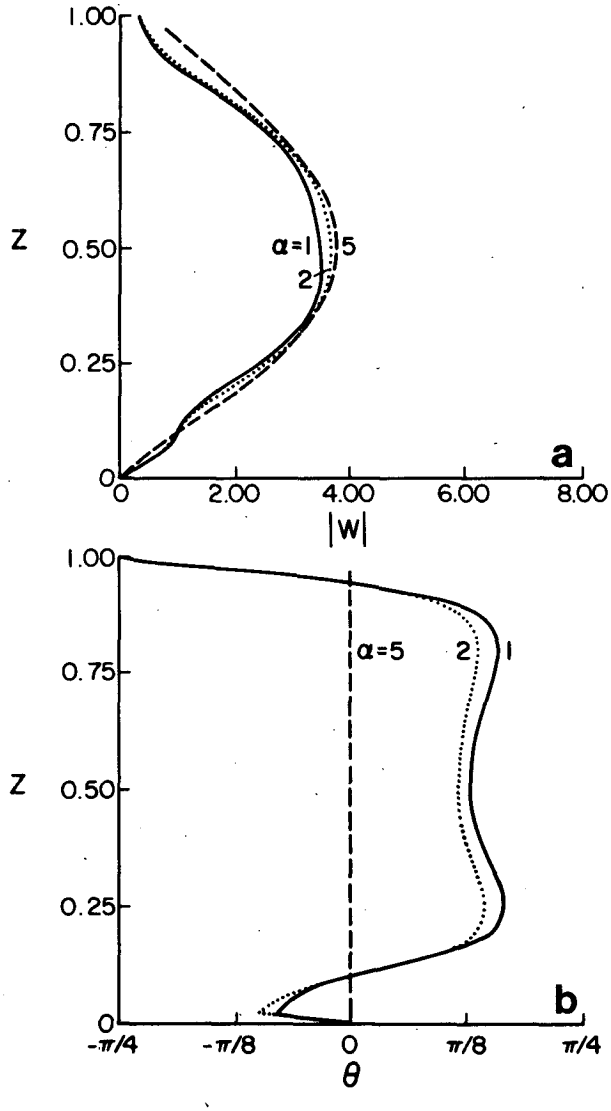

FIG. 10. As in Fig. 3 but for the most unstable wave.

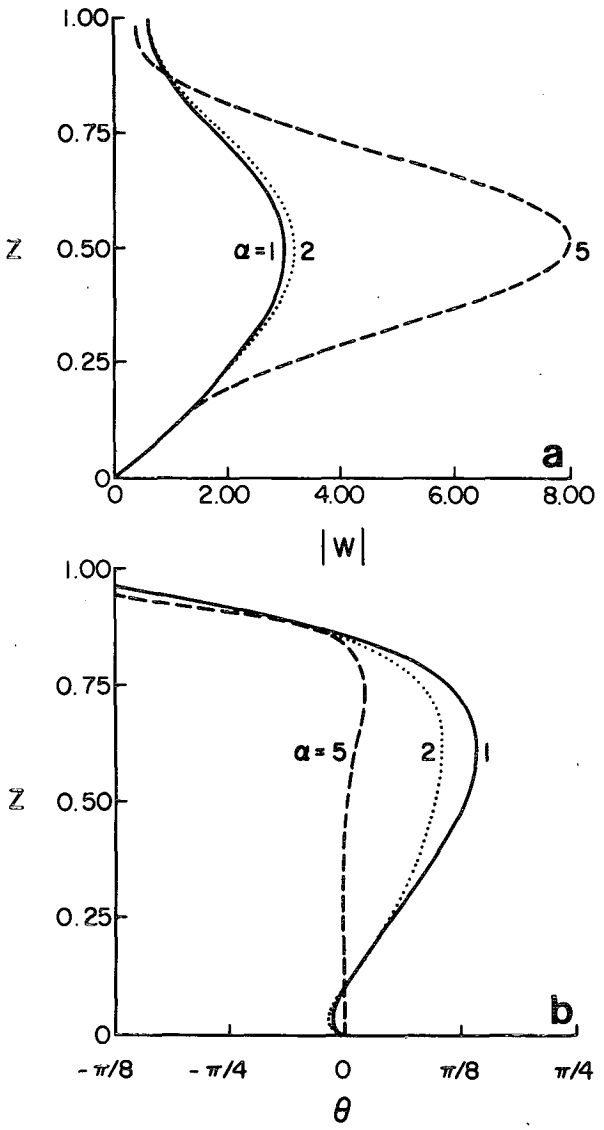

FIG. 11. As in Fig. 3 but for the secondary most unstable wave.

unstable and secondary most-unstable waves was similar. In the most unstable wave the heating was evenly concentrated throughout the convective layer, while in the secondary most-unstable wave it was concentrated near the center of the layer.

In Table 1 a comparison of the properties of the most unstable waves are listed as a function of heating amplitude. In all cases there is a "long" wave with a large group velocity and a "short" wave with a small group velocity. For $\alpha = 1$ or 2, the growth rates of the two waves are the same magnitude, while for $\alpha = 3$ and 5, the long wave has a much higher growth rate. If one considers the associated initial value problem, then in the cases where the two most unstable waves have commensurate growth rates, the wave with the higher group velocity will propagate much more quickly into a region susceptible to CISK and will be the preferred wave.

For waves in the equatorial Pacific, Chang (1976a) estimated that the heating amplitude α was of order 3. For this α the nonhydrostatic wave-CISK model had a preferred scale for growth of 8 km, a doubling time of 6 min, a period of 30 min and a group velocity of 4 m s^{-1}. Due to a drier boundary layer, one would expect α for midlatitude waves to be somewhat smaller than three. For $\alpha = 2$ the nonhydrostatic wave-CISK model had a preferred scale for growth of 6 km, a doubling time of 10 min, a period of 20 min and a group velocity of 2.3 m s^{-1}.

The inclusion of nonhydrostatic effects resulted in a preferred scale for the growth of the waves and eliminated the lack of scale selection inherent in the hydrostatic wave-CISK model. The most unstable wave was characterized by a horizontal length scale of the same order as its vertical extent. Thus, the inclusion of nonhydrostatic effects provides a mechanism by which convection can be organized on the mesoscale. The nonhydrostatic model works because the horizontal and vertical scales are explicitly coupled. Unfortunately, this greatly increases the complexity of the model and results in nonseparable eigenvalue problems for more realistic mean states. Thus one of the key advantages of the parameterization, namely, its simplicity, is lost. An intermediate model, the quasi-hydrostatic approximation, was proposed by Orlanski (1981). By using a series expansion in powers of the aspect ratio, he obtained a first order correction to the hydrostatic approximation. For flows with aspect ratio less than one, the resulting system behaved similarly to the nonhydrostatic one without a great increase in complexity. However, the dynamics responsible for the scale selection in the nonhydrostatic wave-CISK model occur for aspect ratios greater than one and hence will not be captured in a quasi-hydrostatic model. Numerous authors (e.g., Hayashi, 1971; Davies, 1979; Moore, 1983) have included

TABLE 1. Comparison of the properties of the most unstable waves. Length scale used is $H = 5$ km. Brunt-Väisälä frequency used is $N = 10^{-2}$ s^{-1}.

α	H/L	L (km)	ω_i	Doubling time (min)	ω_r	Period (min)	Group velocity (m s^{-1})
1	1.6	3.1	0.06	19	0.75	14	0.8
	4.0	1.2	0.07	16	0.75	14	0.2
2	0.84	6	0.1	10	0.5	20	2.3
	2.4	2.0	0.14	8	0.7	15	0.5
3	0.6	8	0.2	6	0.3	30	4
	1.6	3.1	0.03	38	0.5	20	1
5	0.6	8	0.008	120	0.3	30	4
	0.6	8	0.4	3	0	∞	0

other processes that lead to a coupling between the horizontal and vertical scales in the hydrostatic model. For mesoscale circulations, it would seem that a better route to follow would be the inclusion of nonhydrostatic effects. There still remains the problem of understanding the dynamics responsible for the organization of convection on larger scales. In these cases, the aspect ratio is much less than one and hence the hydrostatic approximation is valid. For this problem, the environment in which the organization develops plays a crucial role in the dynamics. This role has been demonstrated by Raymond (1976) for severe convective storms and Emanuel (1982) for symmetric wave-CISK in a baroclinic flow.

Acknowledgments. The author would like to thank Dr. I. Orlanski for suggesting this problem and the reviewers for their helpful comments. I would also like to thank A. Sousa for typing the manuscript.

REFERENCES

Bolton, D., 1980: Application of Miles theorem to forced linear perturbations. *J. Atmos. Sci.*, **37,** 1639–1642.

Chang, C. P., 1976a: Vertical structure of tropical waves maintained by internally induced cumulus heating. *J. Atmos. Sci.*, **33,** 729–739.

——, 1976b: Comments on "Instability theory of large-scale disturbances in the tropics." *J. Atmos. Sci.*, **33,** 1667–1668.

Charney, J. G., and A. Eliassen, 1964: On the growth of the hurricane depression. *J. Atmos. Sci.*, **21,** 68–75.

Davies, H. C., 1979: Phase-lagged wave-CISK. *Quart. J. Roy. Meteor. Soc.*, **105,** 325–353.

Emanuel, K. A., 1982: Inertial instability and mesoscale convective systems. Part 2: Symmetric CISK in a baroclinic flow. *J. Atmos. Sci.*, **39,** 1080–1097.

Hayashi, Y., 1970: A theory of large-scale equatorial waves generated by condensation heat and accelerating zonal wind. *J. Meteor. Soc. Japan,* **48,** 140–160.

——, 1971: Instability of large-scale equatorial waves with a frequency dependent CISK parameter. *J. Meteor. Soc. Japan,* **49,** 59–62.

Kuo, H. L., 1975: Instability theory of large-scale disturbances in the tropics. *J. Atmos. Sci.*, **32,** 2229–2245.

Lilly, D. K., 1960: On the theory of disturbances in a conditionally unstable atmosphere. *Mon. Wea. Rev.*, **88,** 1–17.

Lindzen, R. S., 1974: Wave-CISK in the tropics. *J. Atmos. Sci.*, **31,** 156–179.

Moore, G. W. K., 1983: On the structure of the narrow cold-frontal rainband. Ph.D. thesis, Princeton University, 141 pp.

Ooyama, K. V., 1964: A dynamical model for the study of tropical cyclone development. *Geofis. Int. (Mexico),* **4,** 187–198.

Orlanski, I., 1981: The quasi-hydrostatic approximation. *J. Atmos. Sci.*, **38,** 572–582.

Raymond, D. J., 1976: Wave-CISK and convective mesosystems. *J. Atmos. Sci.*, **33,** 2392–2398.